Available online at www.sciencedirect.com

ScienceDirect

Nuclear Physics B 910 (2016) 293–308

NUCLEAR PHYSICS B

www.elsevier.com/locate/nuclphysb

Lepton flavor violating decays of neutral higgses in extended mirror fermion model

Chia-Feng Chang [a], Chia-Hung Vincent Chang [b], Chrisna Setyo Nugroho [b], Tzu-Chiang Yuan [c,*]

[a] *Department of Physics, National Taiwan University, Taipei 116, Taiwan*
[b] *Department of Physics, National Taiwan Normal University, Taipei 116, Taiwan*
[c] *Institute of Physics, Academia Sinica, Nangang, Taipei 11529, Taiwan*

Received 12 May 2016; received in revised form 22 June 2016; accepted 7 July 2016

Available online 12 July 2016

Editor: Hong-Jian He

Abstract

We investigate the one-loop induced charged lepton flavor violating decays of the neutral Higgses in an extended mirror fermion model with non-sterile electroweak-scale right-handed neutrinos and a horizontal A_4 symmetry in the lepton sector. It is demonstrated that for the 125 GeV scalar h there is tension between the recent LHC result $\mathcal{B}(h \to \tau\mu) \sim 1\%$ and the stringent limits on the rare processes $\mu \to e\gamma$ and $\tau \to (\mu/e)\gamma$ as well as the muon anomalous magnetic dipole moment Δa_μ from low energy experiments.

1. Motivation

As is well known, the conservation of lepton and baryon numbers are accidental global symmetries in the fundamental Lagrangian of Standard Model (SM). Flavor number conservation, on the other hand, is only a global symmetry of electromagnetism and strong interaction, while weak decays and neutrino oscillations break the flavor symmetry. Moreover, with just one Higgs

* Corresponding author.
E-mail addresses: a29788685@gmail.com (C.-F. Chang), chchang@phy.ntnu.edu.tw (C.-H.V. Chang), setyo13nugros@gmail.com (C.S. Nugroho), tcyuan@phys.sinica.edu.tw (T.-C. Yuan).

http://dx.doi.org/10.1016/j.nuclphysb.2016.07.009

doublet in the SM, the Higgs couplings to the fermions are diagonal at the tree level. Thus in SM, proton decays are strictly forbidden, while $\mu \to e\gamma$, $h \to \tau\mu$, *etc.* can only be induced via weak interaction at loop level. Experimental limits for these processes are indeed very stringent. For example, for the proton lifetime we have the following bound [1]

$$\tau(p \to e^+\gamma) > 670 \times 10^{30} \text{ years}\,, \tag{1}$$

and for the branching fraction of $\mu^+ \to e^+\gamma$ we have the limit from the latest MEG result [2]

$$\mathcal{B}(\mu^+ \to e^+\gamma) < 4.2 \times 10^{-13}\ (90\%\,\text{CL})\,. \tag{2}$$

Search for charged lepton flavor violating (CLFV) Higgs decay $h \to \tau\mu$ at hadron colliders was proposed some time ago [3]. Recently both ATLAS [4] and CMS [5] experiments at the Large Hadron Collider (LHC) have reported the following best fit branching ratios

$$\mathcal{B}(h \to \tau\mu) = \begin{cases} 0.53 \pm 0.51\% \ \text{[ATLAS 8 TeV]}\,, \\ -0.76^{+0.81}_{-0.84}\% \ \text{[CMS 13 TeV]}\,. \end{cases} \tag{3}$$

However, at 95% confidence level (CL), the following upper limits can be deduced

$$\mathcal{B}(h \to \tau\mu) < \begin{cases} 1.43\%\ (95\%\,\text{CL})\ \text{[ATLAS 8 TeV]}\,, \\ 1.20\%\ (95\%\,\text{CL})\ \text{[CMS 13 TeV]}\,. \end{cases} \tag{4}$$

Despite low statistical significance the above best fit results in Eq. (3) are somewhat surprising. Recall that the charged lepton flavor changing Higgs couplings, which may lead to the above decay, are absent at tree level in SM. On the other hand, at one-loop this process can only be induced by the non-vanishing minuscule neutrino masses as implied by various neutrino oscillation experiments and thus the contribution is expected to be quite small. A positive measurement of this branching ratio in the near future at the percent level would be a clear indication of new physics beyond the SM.

Besides we have stringent limits for CLFV radiative decays like $\mu \to e\gamma$ in Eq. (2) as well as

$$\mathcal{B}(\tau \to \mu\gamma) < 4.4 \times 10^{-8}\,, \tag{5}$$

$$\mathcal{B}(\tau \to e\gamma) < 3.3 \times 10^{-8}\,, \tag{6}$$

both at 90% CL from the low energy data of BaBar experiment [6].

In [7], an up-to-date analysis of a previous calculation [8] of $\mu \to e\gamma$ in a class of mirror fermion models with non-sterile electroweak scale right-handed neutrinos [9] was presented for an extension of the models with a horizontal A_4 (the non-abelian discrete symmetry group of the regular tetrahedron) symmetry in the lepton sector [10]. It was demonstrated in [7] that although there exists parameter space relevant to electroweak physics that can accommodate the muon magnetic dipole moment anomaly $\Delta a_\mu = 288(63)(49) \times 10^{-11}$ [1], the current low energy limit Eq. (2) on the branching ratio $\mathcal{B}(\mu \to e\gamma)$ from MEG experiment [2] has disfavored those regions of parameter space.

Over the years, many authors had studied the flavor changing neutral current Higgs decays $h \to \overline{f}_i f_j (i \neq j)$ in both the SM [11] and its various extensions [12–14]. Recently large flux of works on new physics implications for the LHC result of lepton flavor violating Higgs decays Eq. (3) is easily noticed [15–45].

In this work, we present the one-loop calculation of CLFV decay of the neutral Higgses in the extended mirror fermion model [9,10]. In Section 2, we briefly review the extended model and demonstrate that tree level CLFV Higgs couplings are in general present in the model but

Table 1
Lepton and scalar sectors in the extended mirror model and their assignments under A_4.

Fields	$l=(\nu,e)_L^T$	$l^M=(\nu,e^M)_R^T$	e_R	e_L^M	ϕ_{0S}	$\vec{\phi}_S$	Φ	Φ_M	ξ	$\tilde{\chi}$
A_4	**3**	**3**	**3**	**3**	**1**	**3**	**1**	**1**	**1**	**1**

nevertheless highly suppressed by the tiny vacuum expectation values of the singlet scalars which are responsible to the Dirac neutrino masses of order eV. We turn to the one-loop calculation in Section 3 and numerical analysis in Section 4. We conclude in Section 5. Detailed formulas for the loop amplitudes are given in the Appendix.

2. The model and its relevant interactions

In the original mirror fermion model [9], while the gauge group is the same as SM, every left-handed (right-handed) SM fermion has a right-handed (left-handed) mirror partner, and the scalar sector consists of one SM Higgs doublet Φ, one singlet ϕ_{0S} and two triplets ξ (real) and $\tilde{\chi}$ (complex) *á la* Georgi–Machacek [46,47]. One characteristic feature of the model is that the right-handed neutrinos are non-sterile. They are paired up with right-handed mirror charged leptons to form electroweak doublets. This arrangement allows for the electroweak seesaw mechanism [9]: a small vacuum expectation value (VEV) of the scalar singlet ϕ_{0S} provides Dirac masses for the light neutrinos, while a VEV with electroweak size of the Georgi–Machacek triplets provide Majorana masses for the right-handed neutrinos.

Recently, the original model [9] was augmented with an additional mirror Higgs doublet Φ_M in [48] so as to accommodate the 125 GeV Higgs observed at the LHC. In order to avoid flavor changing Yukawa Higgs couplings at the tree level, a global $U(1)_{\rm SM}\times U(1)_{\rm MF}$ symmetry was imposed in the model [48], such that the SM Higgs doublet couples only to the SM fermions while the mirror Higgs doublet couples only to the mirror fermions. Moreover, to achieve the proper vacuum alignment that the SM gauge group $SU(2)_{\rm L}\times U(1)_{\rm Y}$ breaks down into $U(1)_{\rm em}$ correctly without any Nambu–Goldstone boson left over in the physical mass spectrum, a scalar quartic coupling in the potential (the λ_5 term in Eq. (32) of [48]) was introduced. The global symmetry is broken explicitly by this λ_5 term. Electroweak symmetry breaking by the VEVs of the Higgs doublet, mirror Higgs doublet and Georgi–Machacek triplets further breaks this global symmetry. Breaking of this global symmetry will generate tree level CLFV Higgs couplings which we will elaborate further below.

In additional to the original singlet scalar ϕ_{0S}, a A_4 triplet of scalars $\vec{\phi}_S=\{\phi_{1S},\phi_{2S},\phi_{3S}\}$ was introduced in [10] to implement a horizontal family symmetry in the lepton sector which may lead to interesting lepton mixing effects. The three generations of SM leptons and their mirrors are assigned to be triplets of A_4 while the Higgs doublets and the triplets are singlets of A_4. The A_4 assignment of the lepton and scalar sectors are shown in Table 1.

The singlet scalars $\phi_{0S},\vec{\phi}_S$ are the only fields connecting the SM fermions and their mirror counterparts. Recall that A_4 has four irreducible representations **1**, **1**′, **1**″, and **3** with the following multiplication rule[1]:

$$\begin{aligned}\mathbf{3}\times\mathbf{3}=&\mathbf{1}(11+22+33)+\mathbf{1}'(11+\omega^2 22+\omega 33)+\mathbf{1}''(11+\omega 22+\omega^2 33)\\&+\mathbf{3_1}(23,31,12)+\mathbf{3_2}(32,13,21)\end{aligned}\tag{7}$$

[1] Due to the nonabelian nature of A_4, $\mathbf{3_1}$ is differ from $\mathbf{3_2}$.

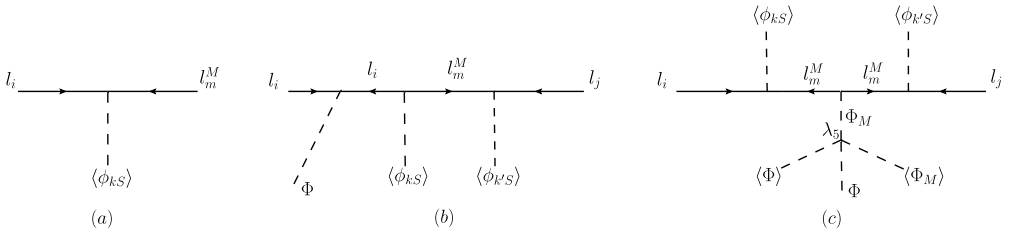

Fig. 1. (a) Tree level mixings between SM and mirror fermions [9]; (b) Tree level CLFV Higgs couplings induced by SM and mirror fermion mixings in the original mirror fermion model [9]; (c) Tree level CLFV Higgs couplings induced by SM and mirror fermion mixings as well as neutral Higgs mixings in the extended mirror fermion model [48].

where $\omega = e^{2\pi i/3}$. In the gauge eigenbasis (fields with superscript 0), one can write down the following A_4 invariant interaction[2]

$$-\mathcal{L}_S = g_{0S}\phi_{0S}(\overline{l_L^0} l_R^{0M})_{\mathbf{1}} + g_{1S}\vec{\phi}_S \cdot (\overline{l_L^0} \times l_R^{0M})_{\mathbf{3_1}} + g_{2S}\vec{\phi}_S \cdot (\overline{l_L^0} \times l_R^{0M})_{\mathbf{3_2}} + \text{H.c.} \tag{8}$$

After the scalar singlets develop VEVs in Eq. (8), they can provide Dirac neutrino mass as mentioned earlier. For example, the first term will give a Dirac neutrino mass $m_D = g_{0S}v_S$ where $v_S = \langle\phi_{0S}\rangle$. Furthermore, they will induce small mixings between SM fermions and their mirrors as well as CLFV Higgs couplings as shown in Figs. 1a, 1b and 1c.

With the complex triplet $\tilde{\chi}$, one can also write down the following A_4 invariant interaction [9,10]

$$\mathcal{L}_T = \frac{1}{2} g_M l_R^{M,T} \sigma_2 \tau_2 \tilde{\chi} l_R^M + \text{H.c.}\,, \tag{9}$$

where both σ_2 and τ_2 are the second Pauli-matrix acting on the Lorentz and $SU(2)_{\text{L}}$ spaces respectively. Eq. (9) then gives

$$-\frac{i}{2} g_M v_R^T \sigma_2 v_R \chi^0 + \cdots . \tag{10}$$

Thus a right-handed neutrino Majorana mass term

$$M_R = g_M v_M \tag{11}$$

can be obtained with $v_M = \langle\chi^0\rangle$, which together with the other two VEVs $v_2 = \langle\Phi\rangle$ and $v_M = \langle\Phi_M\rangle$ play equal role in the electroweak symmetry breaking [48]. Thus the Majorana neutrino mass is linked to the scale of the electroweak symmetry breaking, which is the essence of non-sterile electroweak scale right-handed neutrino model [9]. The magnitude of the light neutrino mass is given by

$$m_\nu = \frac{m_D^2}{M_R} < \mathcal{O}(\text{eV})\,, \tag{12}$$

which implies $v_S \sim 1$ MeV if one takes $g_{0S} \sim 1$ and $M_R \sim 246$ GeV.

One can estimate the induced CLFV Higgs couplings for $h \to \tau\mu$ from Figs. 1b and 1c to be of order $g_S^2 v_S^2/(v_2 M_m)$ and $\lambda_5 g_S^2 v_2 v_S^2/(M_m M_{\Phi_M}^2)$, where M_m and M_{Φ_M} are the masses of the mirror fermion and mirror Higgs doublet respectively. Setting $v_S \sim 1$ MeV, $v_2 \sim M_m \sim M_{\Phi_M} \sim 100$ GeV, and $\lambda_5 \sim g_S \sim 1$, both induced couplings are of order 10^{-10}, which are completely negligible. This is the main rationale to go to one-loop process.

[2] Note that the reality of the Dirac neutrino masses implies $g_{2S} = g_{1S}^*$ [10].

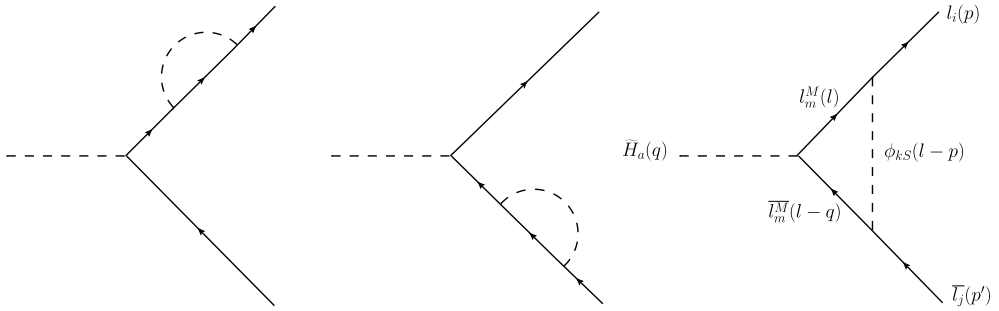

Fig. 2. One-loop induced Feynman diagrams for $\widetilde{H}_a(q) \to l_i(p) + \overline{l}_j(p')$ in EW-scale ν_R model.

We will consider both extensions with A_4 symmetry [10] and mirror Higgs doublet [48] in our calculation. The relevant one-loop Feynman diagram for CLFV Higgs decay in the extended mirror model is shown in Fig. 2. The relevant interactions are all of Yukawa couplings. The first one involving the singlet $\phi_{0S}(k=0)$ and triplet ϕ_{kS} $(k=1,2,3)$ can be expressed as [7]

$$\mathcal{L}_S = -\sum_{k=0}^{3}\sum_{i,m=1}^{3}\left(\bar{l}_{Li}\,\mathcal{U}_{im}^{L\,k}\,l_{Rm}^{M} + \bar{l}_{Ri}\,\mathcal{U}_{im}^{R\,k}\,l_{Lm}^{M}\right)\phi_{kS} + \text{H.c.} \tag{13}$$

where l_{Li} and l_{Ri} are SM leptons, l_{Rm}^{M} and l_{Lm}^{M} are mirror leptons (i, m are generation indices) mass eigenstates relating to their gauge eigenstates according to

$$l_{L,R}^{0} = U_{L,R}^{l}\, l_{L,R} \;, \quad l_{R,L}^{M,0} = U_{R,L}^{l^M}\, l_{R,L}^{M} \;, \tag{14}$$

with unitary matrices $U_{L,R}^{l}$ and $U_{L,R}^{l^M}$; $\mathcal{U}_{im}^{L\,k}$ and $\mathcal{U}_{im}^{R\,k}$ are the coupling coefficients given by

$$\begin{aligned}\mathcal{U}_{im}^{L\,k} &\equiv \left(U_{\text{PMNS}}^{\dagger}\cdot M^{k}\cdot U_{\text{PMNS}}^{l^M}\right)_{im} \;, \\ &= \sum_{j,n=1}^{3}\left(U_{\text{PMNS}}^{\dagger}\right)_{ij} M_{jn}^{k}\left(U_{\text{PMNS}}^{M}\right)_{nm} \;, \end{aligned} \tag{15}$$

$$\begin{aligned}\mathcal{U}_{im}^{R\,k} &\equiv \left(U_{\text{PMNS}}^{\prime\,\dagger}\cdot M^{\prime\,k}\cdot U_{\text{PMNS}}^{\prime\,l^M}\right)_{im} \;, \\ &= \sum_{j,n=1}^{3}\left(U_{\text{PMNS}}^{\prime\,\dagger}\right)_{ij} M_{jn}^{\prime\,k}\left(U_{\text{PMNS}}^{\prime\,M}\right)_{nm} \;, \end{aligned} \tag{16}$$

where the matrix elements for the four matrices $M^k(k=0,1,2,3)$ are listed in Table 2 and $M_{jn}^{\prime\,k}$ can be obtained from M_{jn}^{k} with the following substitutions for the Yukawa couplings $g_{0S} \to g_{0S}^{\prime}$ and $g_{1S} \to g_{1S}^{\prime}$ [7]; U_{PMNS} is the usual neutrino mixing matrix defined as

$$U_{\text{PMNS}} = U_{\nu}^{\dagger} U_{L}^{l} \,, \tag{17}$$

and its mirror and right-handed counter-parts U_{PMNS}^{M}, $U_{\text{PMNS}}^{\prime}$ and $U_{\text{PMNS}}^{\prime M}$ are defined analogously as

$$U_{\text{PMNS}}^{M} = U_{\nu}^{\dagger} U_{R}^{l^M} \,, \tag{18}$$

$$U_{\text{PMNS}}^{\prime} = U_{\nu}^{\dagger} U_{R}^{l} \,, \tag{19}$$

Table 2
Matrix elements for $M^k (k = 0, 1, 2, 3)$ where $\omega \equiv \exp(i2\pi/3)$ and g_{0S} and g_{1S} are Yukawa couplings.

M^k_{jn}	Value
$M^0_{12}, M^0_{13}, M^0_{21}, M^0_{23}, M^0_{31}, M^0_{32}$	0
$M^0_{11}, M^0_{22}, M^0_{33}$	g_{0S}
$M^1_{11}, M^2_{11}, M^3_{11}$	$\frac{2}{3}\mathrm{Re}\,(g_{1S})$
$M^1_{22}, M^2_{22}, M^3_{22}$	$\frac{2}{3}\mathrm{Re}\,(\omega^* g_{1S})$
$M^1_{33}, M^2_{33}, M^3_{33}$	$\frac{2}{3}\mathrm{Re}\,(\omega g_{1S})$
M^1_{12}, M^1_{21}	$\frac{2}{3}\mathrm{Re}\,(\omega g_{1S})$
M^2_{12}, M^3_{21}	$\frac{1}{3}\left(g_{1S} + \omega g^*_{1S}\right)$
M^3_{12}, M^2_{21}	$\frac{1}{3}\left(g^*_{1S} + \omega^* g_{1S}\right)$
M^1_{13}, M^1_{31}	$\frac{2}{3}\mathrm{Re}\,(\omega^* g_{1S})$
M^2_{13}, M^3_{31}	$\frac{1}{3}\left(g_{1S} + \omega^* g^*_{1S}\right)$
M^3_{13}, M^2_{31}	$\frac{1}{3}\left(g^*_{1S} + \omega g_{1S}\right)$
M^1_{23}, M^1_{32}	$\frac{2}{3}\mathrm{Re}\,(g_{1S})$
M^2_{23}, M^3_{32}	$\frac{2\omega^*}{3}\mathrm{Re}\,(g_{1S})$
M^3_{23}, M^2_{32}	$\frac{2\omega}{3}\mathrm{Re}\,(g_{1S})$

and

$$U'^{M}_{\mathrm{PMNS}} = U^{\dagger}_{\nu} U^{l^M}_{L}\,, \tag{20}$$

with

$$U_\nu = U^\nu_L = U^\nu_R = \frac{1}{\sqrt{3}}\begin{pmatrix} 1 & 1 & 1 \\ 1 & \omega^2 & \omega \\ 1 & \omega & \omega^2 \end{pmatrix}. \tag{21}$$

The matrix in Eq. (21) was first discussed by Cabibbo and also by Wolfenstein in the context of CP violation in three generations of neutrino oscillations [49].

The second Yukawa interaction is for the couplings of SM Higgs doublet and the mirror Higgs doublet with the SM fermion pairs and the mirror fermion pairs. It was shown in [48] that the physical neutral Higgs states $(\widetilde{H}_1, \widetilde{H}_2, \widetilde{H}_3)$[3] are in general mixture of the unphysical neutral Higgs states $(H^0_1, H^0_{1M}, H^{0\prime}_1)$ via an orthogonal transformation O:

$$\begin{aligned}\begin{pmatrix} \widetilde{H}_1 \\ \widetilde{H}_2 \\ \widetilde{H}_3 \end{pmatrix} &= \begin{pmatrix} a_{1,1} & a_{1,1M} & a_{1,1'} \\ a_{1M,1} & a_{1M,1M} & a_{1M,1'} \\ a_{1',1} & a_{1',1M} & a_{1',1'} \end{pmatrix} \cdot \begin{pmatrix} H^0_1 \\ H^0_{1M} \\ H^{0\prime}_1 \end{pmatrix} \\ &\equiv O \cdot \begin{pmatrix} H^0_1 \\ H^0_{1M} \\ H^{0\prime}_1 \end{pmatrix}, \end{aligned} \tag{22}$$

where H^0_1 and H^0_{1M} are the neutral components of the SM Higgs and mirror Higgs doublets respectively, and $H^{0\prime}_1$ is linear combination of the neutral components in the Georgi–Machacek

[3] We note that $(\widetilde{H}_1, \widetilde{H}_2, \widetilde{H}_3)$ was denoted as $(\widetilde{H}, \widetilde{H}', \widetilde{H}'')$ respectively in [48].

triplets. The couplings of the physical Higgs $\widetilde{H}_a$ with a pair of SM fermions f and a pair of mirror fermions f^M are given by [48]

$$\mathcal{L}_{\widetilde{H}} = -\frac{g}{2m_W}\sum_{a,f}\widetilde{H}_a\left\{m_f\frac{O_{a1}}{s_2}\overline{f}f + m_{f^M}\frac{O_{a2}}{s_{2M}}\overline{f^M}f^M\right\}, \tag{23}$$

where g is the $SU(2)_L$ weak coupling constant; m_W is the W boson mass; O_{a1} and O_{a2} are the first and second columns of the above orthogonal matrix O in Eq. (22); s_2, s_{2M} and s_M are mixing angles defined by

$$s_2 = \frac{v_2}{v}, \tag{24}$$

$$s_{2M} = \frac{v_{2M}}{v}, \tag{25}$$

$$s_M = \frac{2\sqrt{2}v_M}{v}, \tag{26}$$

with $v = \sqrt{v_2^2 + v_{2M}^2 + 8v_M^2} = 246$ GeV. For the original mirror model [9], one can simply set $\widetilde{H}_1 \to H_1^0 \equiv h$, O_{11}/s_2 and $O_{12}/s_{2M} \to 1$, and drop all other terms with $a \neq 1$ in Eq. (23).

Other information including constraints from the LHC and electroweak precision tests of the extended mirror fermion model can be found in [48].

3. One-loop calculation

The matrix element for the process $\widetilde{H}_a(q) \to l_i(p) + \bar{l}_j(p')$ (Fig. 2) can be written as

$$i\mathcal{M} = i\frac{1}{16\pi^2}\overline{u_i}(p)\left(C_L^{aij}P_L + C_R^{aij}P_R\right)v_j(p'), \tag{27}$$

where $P_{L,R} = (1 \mp \gamma_5)/2$ are the chiral projection operators. In terms of scalar and pseudoscalar couplings the above amplitude can be rewritten as

$$i\mathcal{M} = i\frac{1}{16\pi^2}\overline{u_i}(p)\left(A^{aij} + iB^{aij}\gamma_5\right)v_j(p'), \tag{28}$$

where

$$A^{aij} = \frac{1}{2}\left(C_L^{aij} + C_R^{aij}\right), \quad B^{aij} = \frac{1}{2i}\left(C_R^{aij} - C_L^{aij}\right). \tag{29}$$

The partial decay width is given by

$$\Gamma^{aij} = \frac{1}{2^{11}\pi^5}m_{\widetilde{H}_a}\lambda^{\frac{1}{2}}\left(1, \frac{m_i^2}{m_{\widetilde{H}_a}^2}, \frac{m_j^2}{m_{\widetilde{H}_a}^2}\right) \times\left[|A^{aij}|^2\left(1 - \frac{(m_i+m_j)^2}{m_{\widetilde{H}_a}^2}\right) + |B^{aij}|^2\left(1 - \frac{(m_i-m_j)^2}{m_{\widetilde{H}_a}^2}\right)\right], \tag{30}$$

where $\lambda(x,y,z) = x^2 + y^2 + z^2 - 2(xy + yz + zx)$. The one-loop induced coefficients A^{aij} and B^{aij} are related to C_L^{aij} and C_R^{aij} according to Eq. (29). The formulas for the latter are given in the Appendix. We have ignored the small mixings between the SM and mirror fermions in our one-loop calculation.

The amplitude for $l_i \to l_j\gamma$ $(i \neq j)$ and Δa_i in the extended model can be found in [7].

4. Numerical analysis

We will focus on the case of lightest neutral Higgs $\widetilde{H}_1 \to \tau\mu$ with $\widetilde{H}_1$ identified as the 125 GeV Higgs, and adopt the following strategy which has been used in [7] for the numerical analysis of $\mu \to e\gamma$:

- Two scenarios were specified according to the following forms of the three unknown mixing matrices:
  Scenario 1 (S1): $U'_{\rm PMNS} = U^{M}_{\rm PMNS} = U'^{M}_{\rm PMNS} = U_\nu =$ Eq. (21)
  Scenario 2 (S2): $U'_{\rm PMNS} = U^{M}_{\rm PMNS} = U'^{M}_{\rm PMNS} = U_{\rm PMNS}$, where

$$U^{\rm NH}_{\rm PMNS} = \begin{pmatrix} 0.8221 & 0.5484 & -0.0518 + 0.1439i \\ -0.3879 + 0.07915i & 0.6432 + 0.0528i & 0.6533 \\ 0.3992 + 0.08984i & -0.5283 + 0.05993i & 0.7415 \end{pmatrix}$$

  and

$$U^{\rm IH}_{\rm PMNS} = \begin{pmatrix} 0.8218 & 0.5483 & -0.08708 + 0.1281i \\ -0.3608 + 0.0719i & 0.6467 + 0.04796i & 0.6664 \\ 0.4278 + 0.07869i & -0.5254 + 0.0525i & 0.7293 \end{pmatrix}$$

  for the neutrino masses with normal and inverted hierarchies (NH and IH) respectively. The Majorana phases have been ignored in the analyses. For each scenario, we consider these two possible solutions for the $U_{\rm PMNS}$. Due to the small differences between these two solutions, we expect our results are not too sensitive to the neutrino mass hierarchies.
- All Yukawa couplings g_{0S}, g_{1S}, g'_{0S} and g'_{1S} are assumed to be real. For simplicity, we will assume $g_{0S} = g'_{0S}$, $g_{1S} = g'_{1S}$ and study the following 6 cases:
  (a) $g_{0S} \neq 0,\ g_{1S} = 0$. The A_4 triplet terms are switched off.
  (b) $g_{1S} = 10^{-2} \times g_{0S}$. The A_4 triplet couplings are merely one percent of the singlet ones.
  (c) $g_{1S} = 10^{-1} \times g_{0S}$. The A_4 triplet couplings are 10 percent of the singlet ones.
  (d) $g_{1S} = 0.5 \times g_{0S}$. The A_4 triplet couplings are one half of the singlet ones.
  (e) $g_{1S} = g_{0S}$. Both A_4 singlet and triplet terms have the same weight.
  (f) $g_{0S} = 0,\ g_{1S} \neq 0$. The A_4 singlet terms are switched off.
- For the masses of the singlet scalars ϕ_{kS}, we take

$$m_{\phi_{0S}} : m_{\phi_{1S}} : m_{\phi_{2S}} : m_{\phi_{3S}} = M_S : 2M_S : 3M_S : 4M_S$$

  with a fixed common mass $M_S = 10$ MeV. As long as $m_{\phi_{kS}} \ll m_{l^M_m}$, our results will not be affected much by this assumption.
- For the masses of the mirror lepton l^M_m, we take

$$m_{l^M_m} = M_{\rm mirror} + \delta_m$$

  with $\delta_1 = 0$, $\delta_2 = 10$ GeV, $\delta_3 = 20$ GeV and vary the common mass $M_{\rm mirror}$.
- As shown in [48], the 125 GeV scalar resonance h discovered at the LHC identified as the lightest state $\widetilde{H}_1$ can belong to the *Dr. Jekyll* scenario in which the SM Higgs doublet H^0_1 has a major component or the *Mr. Hyde* scenario in which it is an impostor with H^0_1 only a sub-dominant component. Of all the explicit examples found for both of these scenarios in Ref. [48], we will study the two following cases:

– *Dr. Jekyll* case (Eq. (50) of [48]):

$$O = \begin{pmatrix} 0.998 & -0.0518 & -0.0329 \\ 0.0514 & 0.999 & -0.0140 \\ 0.0336 & 0.0123 & 0.999 \end{pmatrix}, \tag{31}$$

with $\mathrm{Det}(O) = +1$, $m_{\widetilde{H}_1} = 125.7$ GeV, $m_{\widetilde{H}_2} = 420$ GeV, $m_{\widetilde{H}_3} = 601$ GeV, $s_2 = 0.92$, $s_{2M} = 0.16$ and $s_M = 0.36$. In this case,

$$h \equiv \widetilde{H}_1 \sim H_1^0\,, \quad \widetilde{H}_2 \sim H_{1M}^0\,, \quad \widetilde{H}_3 \sim H_1^{0\prime}\,. \tag{32}$$

Hence the 125 GeV Higgs identified as $\widetilde{H}_1$ is composed mainly of the neutral component of the SM doublet in this scenario.

– *Mr. Hyde* case (Eq. (55) of [48]):

$$O = \begin{pmatrix} 0.187 & 0.115 & 0.976 \\ 0.922 & 0.321 & -0.215 \\ 0.338 & -0.940 & 0.046 \end{pmatrix}, \tag{33}$$

with $\mathrm{Det}(O) = -1$, $m_{\widetilde{H}_1} = 125.6$ GeV, $m_{\widetilde{H}_2} = 454$ GeV, $m_{\widetilde{H}_3} = 959$ GeV, $s_2 = 0.401$, $s_{2M} = 0.900$ and $s_M = 0.151$. In this case,

$$h \equiv \widetilde{H}_1 \sim H_1^{0\prime}\,, \quad \widetilde{H}_2 \sim H_1^0\,, \quad \widetilde{H}_3 \sim H_{1M}^0\,. \tag{34}$$

Hence the 125 GeV Higgs identified as $\widetilde{H}_1$ is an impostor in this scenario; it is mainly composed of the two neutral components in the Georgi–Machacek triplets.

In Fig. 3, we plot the contours of the branching ratios $\mathcal{B}(h \to \tau\mu) = 0.53\%$ (red), $\mathcal{B}(\mu \to e\gamma) = 4.2 \times 10^{-13}$ (black), $\mathcal{B}(\tau \to \mu\gamma) = 4.4 \times 10^{-8}$ (blue) and $\mathcal{B}(\tau \to e\gamma) = 3.3 \times 10^{-8}$ (green) on the $(\mathrm{Log}_{10}(M_{\mathrm{mirror}}), \mathrm{Log}_{10}(g_{0S\,\mathrm{or}\,1S}))$ plane for both Scenarios 1 and 2, normal and inverted mass hierarchies and the 6 different cases of the Yukawa couplings (Figs. 3a–3f) in the *Dr. Jekyll* scenario as specified by Eqs. (31)–(32). For the four lines with the same color (hence same process), solid and dashed lines are for Scenario 1 and 2 with normal mass hierarchy (NH) respectively, while dotted and dot-dashed lines are for Scenario 1 and 2 with inverted mass hierarchy (IH) respectively. The orange and yellow bands are the allowed 1σ regions of the experimental and theoretical errors from the muon anomalous magnetic dipole moment in Scenario 1 and 2 respectively, and there are no visible differences between normal and inverted mass hierarchies in these two scenarios for this observable.

Figs. 4a–4f are the same as Figs. 3a–3f respectively but for *Mr. Hyde* scenario as specified by Eqs. (33)–(34).

By studying in details of all the plots in these two figures, we can deduce the following results:

- The bumps at $M_{\mathrm{mirror}} \sim 200$ GeV at all the plots in these two figures are due to large cancellation in the amplitudes between the two one-particle reducible (wave function renormalization) diagrams and the irreducible one-loop diagram shown in Fig. 2. As a result, the Yukawa couplings have to be considerable larger in the contour lines of fixed branching ratios of the processes.
- For the two processes $\tau \to \mu\gamma$ (blue lines) and $\tau \to e\gamma$ (green lines) in all these plots, the solid and dotted lines are coincide to each other while the dashed and dot-dashed lines are very close together. Thus there are essentially no differences between the normal and inverted mass hierarchies in both Scenarios 1 and 2 in these two processes. However, for

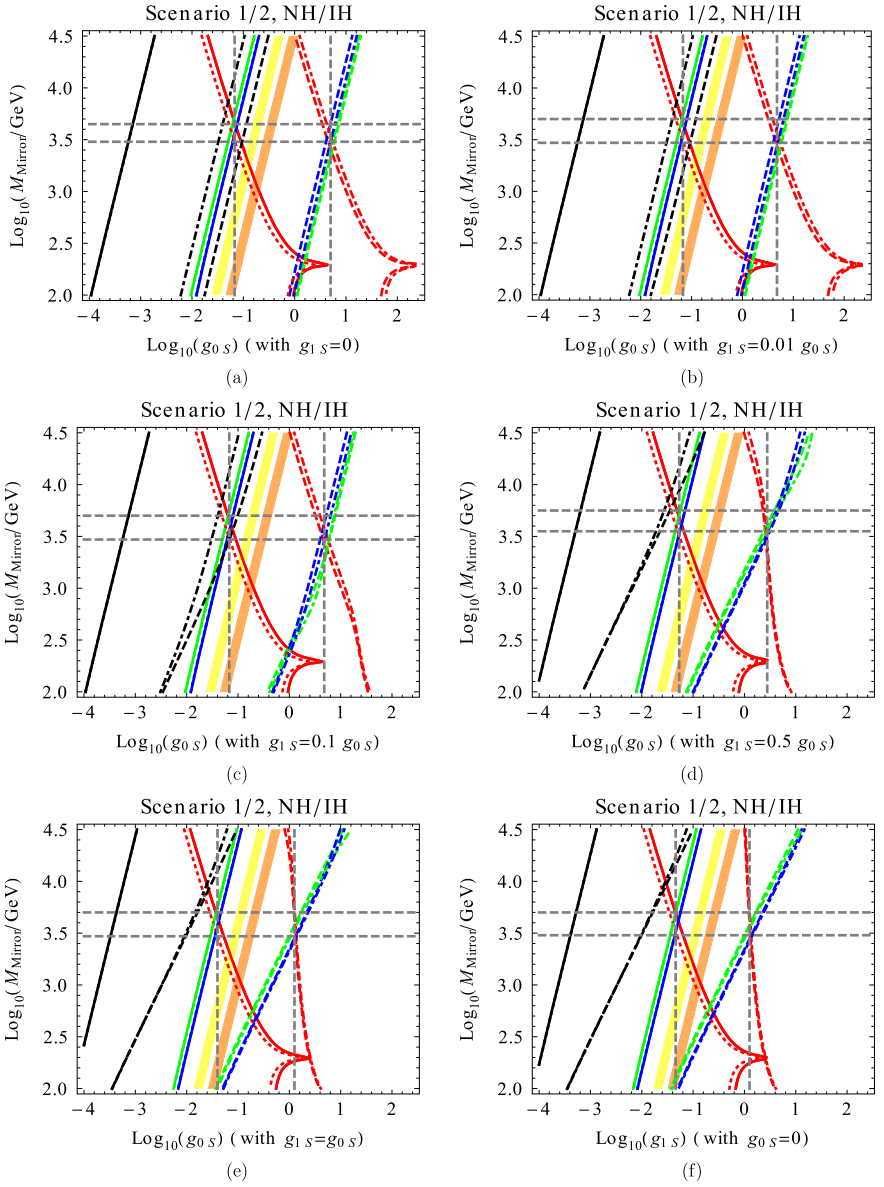

Fig. 3. Contour plots of $\mathcal{B}(h \to \tau\mu) = 0.53\%$ (red), $\mathcal{B}(\mu \to e\gamma) = 4.2 \times 10^{-13}$ (black), $\mathcal{B}(\tau \to \mu\gamma) = 4.4 \times 10^{-8}$ (blue) and $\mathcal{B}(\tau \to e\gamma) = 3.3 \times 10^{-8}$ (green) on the $(\mathrm{Log}_{10}(M_{\mathrm{mirror}}/\mathrm{GeV}), \mathrm{Log}_{10}(g_{0S\,\mathrm{or}\,1S}))$ plane for the *Dr. Jekyll* scenario. Solid/Dotted: NH/IH, S1; Dashed/Dot-dashed: NH/IH, S2; Orange/Yellow band: Δa_μ, S1/S2. (For interpretation of the references to color in this figure legend, the reader is referred to the web version of this article.)

the process $\mu \to e\gamma$ (black lines), only the solid and dotted lines are coincide to each other. Thus there are some differences between normal and inverted mass hierarchies in Scenario 2 but not in Scenario 1 for this process, in particular for cases (a)–(d) in which $g_{1S} \leq 0.5 g_{0S}$.

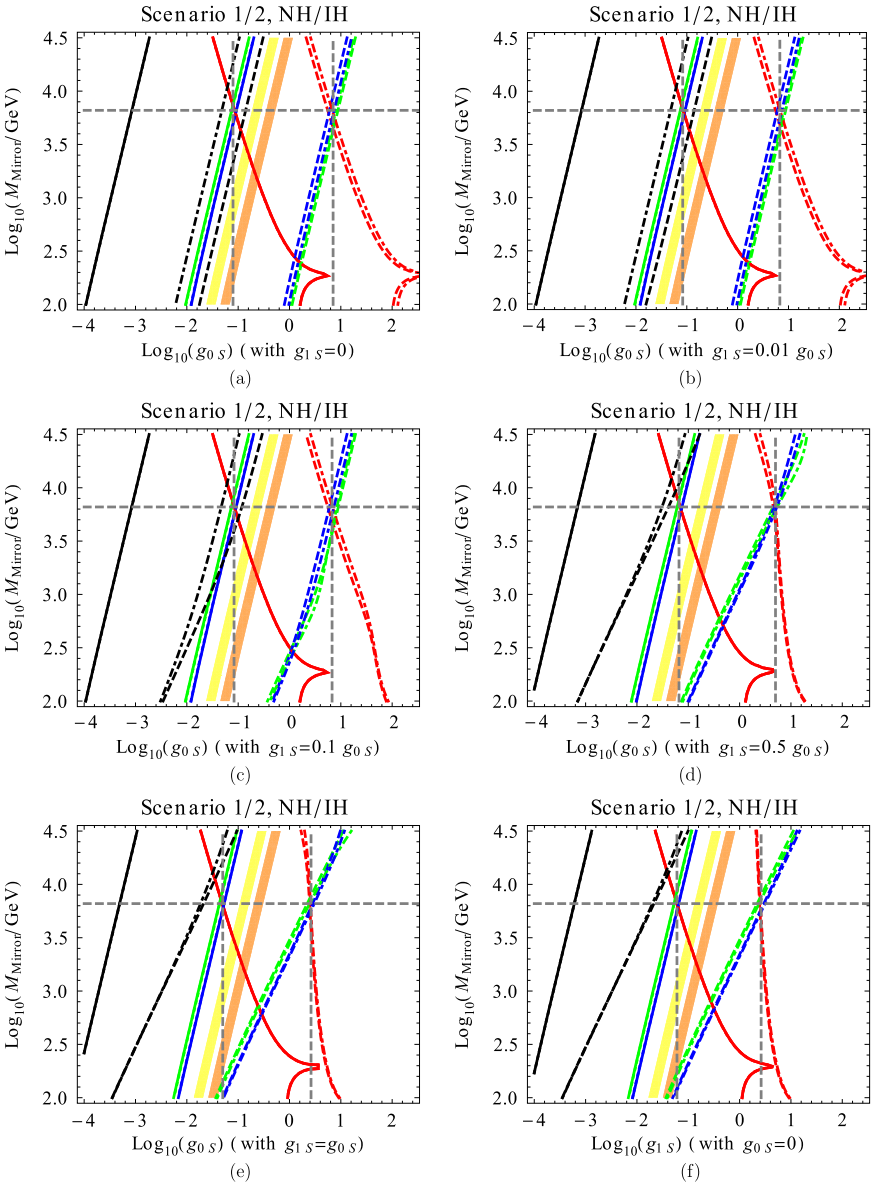

Fig. 4. Same as Fig. 3 but for the *Mr. Hyde* scenario.

- For $h \to \tau\mu$ (red lines), the solid (dashed) and dotted (dot-dashed) lines are either very close (in Fig. 3 for *Dr. Jekyll* scenario) or mostly coincide (in Fig. 4 for *Mr. Hyde* scenario).
- Note that the regions to the right side of the black, blue and green lines in all the plots in these two figures are excluded by the low energy limits of $\mathcal{B}(\mu \to e\gamma)$, $\mathcal{B}(\tau \to \mu\gamma)$ and $\mathcal{B}(\tau \to e\gamma)$ respectively. The ATLAS result of $\mathcal{B}(h \to \tau\mu) = 0.53\%$ (red lines), if not due to statistical fluctuations, is compatible with these low energy limits only if there are intersection points of the red lines with the corresponding black, blue and green lines.

Table 3
The upper (lower) limit of Yukawa couplings (mirror fermion masses) deduced from the LHC result of $\mathcal{B}(h \to \tau\mu)$ as compared with CLFV decays $l_i \to l_j\gamma$ and the 1σ corridor of Δa_μ.

Mode	Quantity	Scenario 1		Scenario 2	
		Dr. Jekyll	*Mr. Hyde*	*Dr. Jekyll*	*Mr. Hyde*
$\tau \to (\mu, e)\gamma$	Mass (TeV)	4.46	6.61	2.95	6.61
	$g_{0S}(g_{1S})$	0.0676	0.0832	5.01	6.76
$\mu \to e\gamma$	Mass (TeV)	~ 100	$> 10^{2.5}$	~ 95	$> 10^{2.5}$
	$g_{0S}(g_{1S})$	$10^{-2.6}$	$10^{-2.1}$	0.063	0.117
Δa_μ	Mass (TeV)	$1.17^{+0.35}_{-0.25}$	$1.58^{+0.50}_{-0.18}$	~ 95	$> 10^{2.5}$
	$g_{0S}(g_{1S})$	$0.16^{+0.08}_{-0.03}$	$0.19^{+0.05}_{-0.04}$	~ 0.66	~ 1

Take Fig. 3a as an example. For the case of *Dr. Jekyll* in Scenario 1, the solid (or dotted) red line intersects with the solid (or dotted) blue and green lines at $M_{\text{mirror}} \sim 4.47$ TeV where $g_{0S} \sim 0.07$. In Scenario 2, the dashed (or dot-dashed) red line intersects the dashed (or dot-dashed) blue or green lines at $M_{\text{mirror}} \sim 3.55$ TeV with a considerable larger $g_{0S} \sim 5$. For the black lines from the most stringent limit of $\mu \to e\gamma$, their intersections with the red lines are well beyond 10 TeV for the mirror lepton masses. Similar statements can be obtained from the other plots in these two figures. From these intersections in these figures, one can deduce the lower (upper) limits of the mirror fermion masses (couplings) which we summarize in Table 3. Such a large mirror lepton mass M_{mirror} or coupling g_{0S} indicates a break down of the perturbative calculation and/or violation of unitarity. However taking what we have literally there is tension between the large branching ratio $\mathcal{B}(h \to \tau\mu)$ of 1% from LHC and the low energy limits of $\mathcal{B}(\tau \to (\mu, e)\gamma)$ and $\mathcal{B}(\mu \to e\gamma)$, in particular the latter one.

- Since all the four black lines for the process $\mu \to e\gamma$ are located outside to the left of the orange and yellow bands of Δa_μ in all these plots, one can not accommodate both $\mu \to e\gamma$ and Δa_μ in the present context of this model. On the other hand, for each of the other three processes, it is possible to do so depending on the scenarios and neutrino mass hierarchies. For instance, from Fig. 3a, we can see that for $h \to \tau\mu$, the red solid or dotted line passes through the orange band in Scenario 1 in the region of $0.16 < g_{0S} < 0.2$ and 794 GeV $< M_{\text{Mirror}} < 1.5$ TeV, while the intersection of the red dash or dot-dashed line with the yellow band in scenario 2 is located at large mirror fermion mass and large Yukawa coupling, as shown in the last 2 rows in Table 3. For the other two processes $\tau \to \mu\gamma$ and $\tau \to e\gamma$ the intersections are possible in Scenario 2 but not in Scenario 1. Similar results can be deduced for the other cases of Yukawa couplings in Figs. 3 and 4.
- In the event that the LHC result in Eq. (3) is just a statistical fluctuation,[4] the limits in Eq. (4) will be improved further in LHC Run 2. The red contour lines would be shifted toward to the left side of the current ones in the two Figs. 3 and 4. Their intersections with the black, blue and green lines would then be at lower mirror lepton masses and smaller Yukawa couplings, since the low energy limits of the CLFV decays $l_i \to l_j\gamma$ are unlikely to be changed significantly anytime soon. Certainly this would alleviate the tension mentioned above.

[4] The negative branching ratio in Eq. (3) from CMS suggested that it may well be so.

5. Conclusion

To summarize, LHC has reported excess in the charged lepton flavor violating Higgs decay $h \to \tau\mu$ at about 2σ level. More data is needed to collect at Run 2 so as to confirm whether these are indeed true signals or simply statistical fluctuations.

If the branching ratio of $h \to \tau\mu$ is indeed at the percent level, new physics associated with lepton flavor violation may be at a scale not too far from the electroweak scale. Crucial question is whether in a new physics model this large branching ratio of $h \to \tau\mu$ is compatible with the current low energy limits of $\tau \to \mu\gamma$ and $\tau \to e\gamma$ from Belle experiments, the most stringent limit of $\mu \to e\gamma$ from MEG experiment, and the muon anomalous magnetic dipole moment.

We analyze these charged lepton flavor violating processes in the context of an extended mirror fermion model with non-sterile electroweak scale right-handed neutrinos as well as a horizontal A_4 symmetry imposed on the lepton sector. We found that the masses of the mirror lepton fermions entering the loops of these processes play a central role. These masses can be of the order of a few hundred GeV to a few TeV depending on the sizes of the Yukawa couplings among the leptons, mirror leptons and the scalar singlets in the model as well as whether or not the 125 GeV scalar boson is a Higgs impostor and which scenario one assumes for the three unknown PMNS-type mixing matrices. We demonstrate that in general there is tension between the LHC result and the low energy limits since these results are compatible only if the mirror lepton masses are quite heavy and/or the Yukawa couplings involving the scalar singlets are large.

Lastly, we comment on the possible collider signals for the mirror fermions [50]. Mirror leptons if not too heavy can be produced at the LHC via electroweak processes [9], *e.g.* $q\bar{q} \to Z \to l_R^M \overline{l_R^M}$, $\nu_R \overline{\nu_R}$ and $q\overline{q'} \to W^{\mp} \to l_R^M \overline{\nu_R}, \nu_R \overline{l_R^M}$. The mirror lepton decays as $l_R^M \to l_L + \phi_S$ or $l_R^M \to \nu_R + W^{-(*)}$ for $m_{l_R^M} > m_{\nu_R}$ plus the conjugate processes, while the right-handed neutrino can decay as $\nu_R \to \nu_L + \phi_S$ or $\nu_R \to l_R^M + W^{+(*)}$ for $m_{\nu_R} > m_{l_R^M}$ followed by $l_R^M \to l_L + \phi_S$. If kinematics allowed, the scalar singlet ϕ_S can decay into lepton pair as well through mixings; otherwise they would appear as missing energies like neutrinos. Thus the signals at the LHC or future 100 TeV SPPC would be multiple lepton pairs plus missing energies. In the case where the right-handed neutrinos are Majorana fermions, we would have same sign dilepton plus missing energies. Assuming $l_R^M \to l_L + \phi_S$ is the dominant mode and the Yukawa couplings are small enough, the decay length of the mirror lepton could be as large as a few millimeter [50]. Thus the mirror lepton may lead to a displaced vertex and decay outside the beam pipe. These leptonic final states may have been discarded by the current algorithms adopted by the LHC experiments. It is therefore quite important for the experimentalists to devise new algorithms to search for these mirror fermions that may decay outside the beam pipe.

The scale of new physics may be hidden in the lepton flavor violating processes like $h \to \tau(\mu, e)$, $\tau \to (\mu, e)\gamma$, $\mu \to e\gamma$, $\mu \to eee$, μ-e conversion *etc.* Ongoing and future experiments at high energy and high intensity frontiers could shed light in the mirror fermion model that may be responsible to these lepton flavor violating processes.

Acknowledgements

We would like to thank Wei-Chih Huang and P.Q. Hung for useful discussions. This work is supported by the Ministry of Science and Technology of Taiwan (MoST) under grant 104-2112-M-001-001-MY3.

Appendix

The dimensionless coefficients C_L^{aij} and C_R^{aij} defined in Eq. (28) are given by

$$
\begin{aligned}
C_L^{aij} = & \frac{g O_{a1}}{2 s_2 m_W (m_i^2 - m_j^2)} \sum_{k,m} \int_0^1 dx \left\{ \left[(1-x) \left(m_i m_j^2 \mathcal{U}_{im}^{Lk} \left(\mathcal{U}_{mj}^{Lk} \right)^* + m_j m_i^2 \mathcal{U}_{im}^{Rk} \left(\mathcal{U}_{mj}^{Rk} \right)^* \right) \right. \right. \\
& \left. \left. + m_i m_j M_m \mathcal{U}_{im}^{Lk} \left(\mathcal{U}_{mj}^{Rk} \right)^* \right] \log \left(\frac{\Delta_1}{\Delta_2} \right) + M_m \mathcal{U}_{im}^{Rk} \left(\mathcal{U}_{mj}^{Lk} \right)^* \left(m_i^2 \log \Delta_1 - m_j^2 \log \Delta_2 \right) \right\} \\
& + \frac{g O_{a2}}{2 s_{2M} m_W} \sum_{k,m} M_m \mathcal{U}_{im}^{Rk} \left(\mathcal{U}_{mj}^{Lk} \right)^* \left(-\frac{1}{2} - 2 \int_0^1 dx \int_0^{1-x} dy \log \Delta_3 \right) \\
& - \frac{g O_{a2}}{2 s_{2M} m_W} \sum_{k,m} M_m \int_0^1 dx \int_0^{1-x} dy \frac{1}{\Delta_3} \left\{ (1-2y) \frac{m_i M_m}{m_{\widetilde{H}_a}^2} \mathcal{U}_{im}^{Lk} \left(\mathcal{U}_{mj}^{Lk} \right)^* \right. \\
& + (1-2x) \frac{m_j M_m}{m_{\widetilde{H}_a}^2} \mathcal{U}_{im}^{Rk} \left(\mathcal{U}_{mj}^{Rk} \right)^* + (1-x-y) \frac{m_i m_j}{m_{\widetilde{H}_a}^2} \mathcal{U}_{im}^{Lk} \left(\mathcal{U}_{mj}^{Rk} \right)^* \\
& \left. - \left[xy + (1-x-y)(y r_i + x r_j) - r_m \right] \mathcal{U}_{im}^{Rk} \left(\mathcal{U}_{mj}^{Lk} \right)^* \right\}, \qquad (35)
\end{aligned}
$$

C_R^{aij} can be obtained from C_L^{aij} simply by substituting $\mathcal{U}^L \leftrightarrow \mathcal{U}^R$, namely

$$
\begin{aligned}
C_R^{aij} = & \frac{g O_{a1}}{2 s_2 m_W (m_i^2 - m_j^2)} \sum_{k,m} \int_0^1 dx \left\{ \left[(1-x) \left(m_i m_j^2 \mathcal{U}_{im}^{Rk} \left(\mathcal{U}_{mj}^{Rk} \right)^* + m_j m_i^2 \mathcal{U}_{im}^{Lk} \left(\mathcal{U}_{mj}^{Lk} \right)^* \right) \right. \right. \\
& \left. \left. + m_i m_j M_m \mathcal{U}_{im}^{Rk} \left(\mathcal{U}_{mj}^{Lk} \right)^* \right] \log \left(\frac{\Delta_1}{\Delta_2} \right) + M_m \mathcal{U}_{im}^{Lk} \left(\mathcal{U}_{mj}^{Rk} \right)^* \left(m_i^2 \log \Delta_1 - m_j^2 \log \Delta_2 \right) \right\} \\
& + \frac{g O_{a2}}{2 s_{2M} m_W} \sum_{k,m} M_m \mathcal{U}_{im}^{Lk} \left(\mathcal{U}_{mj}^{Rk} \right)^* \left(-\frac{1}{2} - 2 \int_0^1 dx \int_0^{1-x} dy \log \Delta_3 \right) \\
& - \frac{g O_{a2}}{2 s_{2M} m_W} \sum_{k,m} M_m \int_0^1 dx \int_0^{1-x} dy \frac{1}{\Delta_3} \left\{ (1-2y) \frac{m_i M_m}{m_{\widetilde{H}_a}^2} \mathcal{U}_{im}^{Rk} \left(\mathcal{U}_{mj}^{Rk} \right)^* \right. \\
& + (1-2x) \frac{m_j M_m}{m_{\widetilde{H}_a}^2} \mathcal{U}_{im}^{Lk} \left(\mathcal{U}_{mj}^{Lk} \right)^* + (1-x-y) \frac{m_i m_j}{m_{\widetilde{H}_a}^2} \mathcal{U}_{im}^{Rk} \left(\mathcal{U}_{mj}^{Lk} \right)^* \\
& \left. - \left[xy + (1-x-y)(y r_i + x r_j) - r_m \right] \mathcal{U}_{im}^{Lk} \left(\mathcal{U}_{mj}^{Rk} \right)^* \right\}. \qquad (36)
\end{aligned}
$$

The Δ_1, Δ_2 and Δ_3 are given by

$$\Delta_1 = x r_m + (1-x) r_k - x(1-x) r_j - i 0^+ , \qquad (37)$$

$$\Delta_2 = x r_m + (1-x) r_k - x(1-x) r_i - i 0^+ , \qquad (38)$$

$$\Delta_3 = (x+y)r_m + (1-x-y)(r_k - yr_i - xr_j) - xy - i0^+ . \tag{39}$$

Here $r_m = M_m^2/m_{\widetilde{H}_a}^2$, $r_{i,j} = m_{i,j}^2/m_{\widetilde{H}_a}^2$ and $r_k = m_k^2/m_{\widetilde{H}_a}^2$ with M_m, $m_{i,j}$ and m_k denoting the masses of the mirror leptons, leptons and scalar singlets respectively.

References

[1] K.A. Olive, et al., Particle Data Group, Chin. Phys. C 38 (2014) 090001 and (2015) update.
[2] A.M. Baldini, et al., MEG Collaboration, arXiv:1605.05081 [hep-ex].
[3] T. Han, D. Marfatia, Phys. Rev. Lett. 86 (2001) 1442, arXiv:hep-ph/0008141.
[4] G. Aad, et al., ATLAS Collaboration, arXiv:1604.07730 [hep-ex].
[5] See the talk by M. Cepeda at Higgs tasting workshop 2016, Benasque, Spain, https://indico.cern.ch/event/527663/contributions/2168318/attachments/1274703/1893958/Cepeda.pdf.
[6] B. Aubert, et al., BaBar Collaboration, Phys. Rev. Lett. 104 (2010) 021802, arXiv:0908.2381 [hep-ex].
[7] P.Q. Hung, T. Le, V.Q. Tran, T.C. Yuan, J. High Energy Phys. 1512 (2015) 169, arXiv:1508.07016 [hep-ph].
[8] P.Q. Hung, Phys. Lett. B 659 (2008) 585, arXiv:0711.0733 [hep-ph].
[9] P.Q. Hung, Phys. Lett. B 649 (2007) 275, arXiv:hep-ph/0612004.
[10] P.Q. Hung, T. Le, J. High Energy Phys. 1509 (2015) 001, J. High Energy Phys. 1509 (2015) 134, arXiv:1501.02538 [hep-ph].
[11] L.G. Benitez-Guzmán, I. García-Jiménez, M.A. López-Osorio, E. Martínez-Pascual, J.J. Toscano, J. Phys. G 42 (2015) 085002, arXiv:1506.02718 [hep-ph].
[12] A. Pilaftsis, Phys. Lett. B 285 (1992) 68.
[13] J.G. Korner, A. Pilaftsis, K. Schilcher, Phys. Rev. D 47 (1993) 1080, arXiv:hep-ph/9301289.
[14] J.L. Diaz-Cruz, J.J. Toscano, Phys. Rev. D 62 (2000) 116005, arXiv:hep-ph/9910233.
[15] I. Doršner, S. Fajfer, A. Greljo, J.F. Kamenik, N. Košnik, I. Nišandžic, J. High Energy Phys. 1506 (2015) 108, arXiv:1502.07784 [hep-ph].
[16] X.F. Han, L. Wang, J.M. Yang, Phys. Lett. B 757 (2016) 537, arXiv:1601.04954 [hep-ph].
[17] M. Sher, K. Thrasher, Phys. Rev. D 93 (5) (2016) 055021, arXiv:1601.03973 [hep-ph].
[18] M. Buschmann, J. Kopp, J. Liu, X.P. Wang, arXiv:1601.02616 [hep-ph].
[19] A. Crivellin, G. D'Ambrosio, M. Hoferichter, L.C. Tunstall, Phys. Rev. D 93 (7) (2016) 074038, arXiv:1601.00970 [hep-ph];
A. Crivellin, J. Heeck, P. Stoffer, Phys. Rev. Lett. 116 (8) (2016) 081801, arXiv:1507.07567 [hep-ph];
A. Crivellin, G. D'Ambrosio, J. Heeck, Phys. Rev. D 91 (7) (2015) 075006, arXiv:1503.03477 [hep-ph];
A. Crivellin, G. D'Ambrosio, J. Heeck, Phys. Rev. Lett. 114 (2015) 151801, arXiv:1501.00993 [hep-ph].
[20] N. Bizot, S. Davidson, M. Frigerio, J.-L. Kneur, J. High Energy Phys. 1603 (2016) 073, arXiv:1512.08508 [hep-ph].
[21] L.T. Hue, H.N. Long, T.T. Thuc, T. Phong Nguyen, Nucl. Phys. B 907 (2016) 37, arXiv:1512.03266 [hep-ph].
[22] J.M. Cline, Phys. Rev. D 93 (7) (2016) 075017, arXiv:1512.02210 [hep-ph].
[23] H.B. Zhang, T.F. Feng, S.M. Zhao, Y.L. Yan, F. Sun, arXiv:1511.08979 [hep-ph].
[24] Y. Omura, E. Senaha, K. Tobe, arXiv:1511.08880 [hep-ph];
Y. Omura, E. Senaha, K. Tobe, J. High Energy Phys. 1505 (2015) 028, arXiv:1502.07824 [hep-ph].
[25] R. Benbrik, C.H. Chen, T. Nomura, Phys. Rev. D 93 (9) (2016) 095004, arXiv:1511.08544 [hep-ph].
[26] D. Aloni, Y. Nir, E. Stamou, J. High Energy Phys. 1604 (2016) 162, arXiv:1511.00979 [hep-ph].
[27] E. Arganda, M.J. Herrero, R. Morales, A. Szynkman, J. High Energy Phys. 1603 (2016) 055, arXiv:1510.04685 [hep-ph].
[28] Y. Cai, M.A. Schmidt, J. High Energy Phys. 1602 (2016) 176, arXiv:1510.02486 [hep-ph].
[29] S. Baek, Z.F. Kang, J. High Energy Phys. 1603 (2016) 106, arXiv:1510.00100 [hep-ph].
[30] X. Chen, L. Xia, arXiv:1509.08149 [hep-ph].
[31] S. Baek, K. Nishiwaki, Phys. Rev. D 93 (1) (2016) 015002, arXiv:1509.07410 [hep-ph].
[32] N. Košnik, arXiv:1509.04590 [hep-ph].
[33] X. Liu, L. Bian, X.Q. Li, J. Shu, Nucl. Phys. B 909 (2016) 507, arXiv:1508.05716 [hep-ph].
[34] F.J. Botella, G.C. Branco, M. Nebot, M.N. Rebelo, Eur. Phys. J. C 76 (3) (2016) 161, arXiv:1508.05101 [hep-ph].
[35] E. Arganda, M.J. Herrero, X. Marcano, C. Weiland, Phys. Rev. D 93 (5) (2016) 055010, arXiv:1508.04623 [hep-ph].
[36] Y.n. Mao, S.h. Zhu, Phys. Rev. D 93 (3) (2016) 035014, arXiv:1505.07668 [hep-ph].
[37] B. Altunkaynak, W.S. Hou, C. Kao, M. Kohda, B. McCoy, Phys. Lett. B 751 (2015) 135, arXiv:1506.00651 [hep-ph].

[38] X.G. He, J. Tandean, Y.J. Zheng, J. High Energy Phys. 1509 (2015) 093, arXiv:1507.02673 [hep-ph].
[39] C.W. Chiang, H. Fukuda, M. Takeuchi, T.T. Yanagida, J. High Energy Phys. 1511 (2015) 057, arXiv:1507.04354 [hep-ph].
[40] W. Altmannshofer, S. Gori, A.L. Kagan, L. Silvestrini, J. Zupan, Phys. Rev. D 93 (3) (2016) 031301, arXiv:1507.07927 [hep-ph].
[41] K. Cheung, W.Y. Keung, P.Y. Tseng, Phys. Rev. D 93 (1) (2016) 015010, arXiv:1508.01897 [hep-ph].
[42] D. Das, A. Kundu, Phys. Rev. D 92 (1) (2015) 015009, arXiv:1504.01125 [hep-ph].
[43] J. Heeck, M. Holthausen, W. Rodejohann, Y. Shimizu, Nucl. Phys. B 896 (2015) 281, arXiv:1412.3671 [hep-ph].
[44] D. Aristizabal Sierra, A. Vicente, Phys. Rev. D 90 (11) (2014) 115004, arXiv:1409.7690 [hep-ph].
[45] R. Harnik, J. Kopp, J. Zupan, J. High Energy Phys. 1303 (2013) 026, arXiv:1209.1397 [hep-ph].
[46] H. Georgi, M. Machacek, Nucl. Phys. B 262 (1985) 463.
[47] M.S. Chanowitz, M. Golden, Phys. Lett. B 165 (1985) 105.
[48] V. Hoang, P.Q. Hung, A.S. Kamat, Nucl. Phys. B 896 (2015) 611–656, arXiv:1412.0343 [hep-ph].
[49] N. Cabibbo, Phys. Lett. B 72 (1978) 333;
L. Wolfenstein, Phys. Rev. D 18 (1978) 958.
[50] S. Chakdar, K. Ghosh, V. Hoang, P.Q. Hung, S. Nandi, Phys. Rev. D 93 (2016) 035007, arXiv:1508.07318 [hep-ph].